Structure
Article

Structure of the Yeast WD40 Domain Protein Cia1, a Component Acting Late in Iron-Sulfur Protein Biogenesis

Vasundara Srinivasan,[1,3] Daili J.A. Netz,[2] Holger Webert,[2] Judita Mascarenhas,[2] Antonio J. Pierik,[2] Hartmut Michel,[1] and Roland Lill[2,*]
[1]Department of Molecular Membrane Biology, Max-Planck Institute for Biophysics, Max-von-Laue Str. 3, D-60438 Frankfurt/M, Germany
[2]Institut für Zytobiologie, Philipps Universität Marburg, Robert-Koch Str. 6, D-35033 Marburg, Germany
[3]Present address: Department of Molecular and Cellular Interactions, VIB, Pleinlaan 2, 1050 Brussels, Belgium.
*Correspondence: lill@staff.uni-marburg.de
DOI 10.1016/j.str.2007.08.009

SUMMARY

The WD40-repeat protein Cia1 is an essential, conserved member of the cytosolic iron-sulfur (Fe/S) protein assembly (CIA) machinery in eukaryotes. Here, we report the crystal structure of *Saccharomyces cerevisiae* Cia1 to 1.7 Å resolution. The structure folds into a β propeller with seven blades pseudo symmetrically arranged around a central axis. Structure-based sequence alignment of Cia1 proteins shows that the WD40 propeller core elements are highly conserved. Site-directed mutagenesis of amino acid residues in loop regions with high solvent accessibility identified that the conserved top surface residue R127 performs a critical function: the R127 mutant cells grew slowly and were impaired in cytosolic Fe/S protein assembly. Human Ciao1, which reportedly interacts with the Wilms' tumor suppressor, WT1, is structurally similar to yeast Cia1. We show that Ciao1 can functionally replace Cia1 and support cytosolic Fe/S protein biogenesis. Hence, our structural and biochemical studies indicate the conservation of Cia1 function in eukaryotes.

INTRODUCTION

Iron-sulfur (Fe/S) clusters are versatile, ancient cofactors of proteins that are involved in electron transport, enzyme catalysis, and the regulation of gene expression (Beinert et al., 1997). The synthesis of Fe/S clusters and their insertion into apoproteins involves the function of complex cellular assemblies. In non-plant eukaryotes, (Fe/S) proteins are present in mitochondria, the cytosol, and the nucleus. Mitochondria are the primary site of Fe/S protein formation, since they have been shown to be essential for the maturation of both mitochondrial and extramitochondrial Fe/S proteins (Lill and Mühlenhoff, 2005, 2006; Rouault and Tong, 2005). The assembly of Fe/S clusters in mitochondria is mediated by the Fe/S cluster assembly machinery that consists of at least 14 proteins. While the basic concepts of this process have been elucidated, the molecular mechanisms underlying Fe/S protein assembly in the cytosol and the nucleus are still poorly understood. Cytosolic proteins involved in Fe/S protein assembly have been characterized only recently. The two related P loop NTPases termed Cfd1 (Roy et al., 2003) and Nbp35 (Hausmann et al., 2005) form a complex and serve as a scaffold for transient Fe/S cluster assembly before cluster transfer to apoproteins (Netz et al., 2007). This latter process requires a protein designated Nar1 (Balk et al., 2004), which exhibits similarity to bacterial and algal iron-only hydrogenases, as well as the WD40-repeat protein Cia1 (Balk et al., 2005). The four proteins form the CIA (cytosolic Fe/S protein assembly) machinery, are located in both the cytosol and the nucleus, and are essential for cell viability in yeast and *Drosophila melanogaster* (Radford et al., 2005). Homologs of all of these proteins are present in virtually all eukaryotes sequenced to date (e.g., fungi, mammals, plants, and parasites [Lill and Mühlenhoff, 2005]). Their downregulation in yeast *Saccharomyces cerevisiae* leads to similar phenotypical consequences, including growth retardation and severe maturation defects of cytosolic and nuclear, but not mitochondrial, Fe/S proteins. The CIA proteins are also essential for the incorporation of Fe/S clusters at the N terminus of Rli1, an essential protein that plays a crucial role in the export of ribosomal subunits from the nucleus and in translation initiation (Dong et al., 2004; Kispal et al., 2005; Yarunin et al., 2005).

The most recently identified CIA component is Cia1, which is encoded as a fusion protein with the P loop NTPase Cfd1 in *Schizosaccharomyces pombe* (Balk et al., 2005). While enzyme activity and in vivo ^{55}Fe incorporation measurements have verified that *S. cerevisiae* Cia1 is involved in the maturation of cytosolic and nuclear, but not mitochondrial, Fe/S proteins (Balk et al., 2005), other properties strikingly differ from those of the other three CIA proteins. Cia1 is the only CIA component that is not required for the assembly of the Fe/S clusters on the other CIA proteins, Cfd1, Nbp35, and Nar1, suggesting a specific function in cluster transfer to target proteins,

Table 1. Data Collection, Phasing, and Refinement Statistics

Data Set	Native	Se-Met
Beamline	SLS	EMBL, Hamburg
Wavelength (Å)	0.931	0.976
Space group	$P2_12_12_1$	$P2_12_12_1$
Cell dimensions		
a	34.711	35.699
b	68.914	71.450
c	129.40	131.169
α	90	90
β	90	90
γ	90	90
Resolution range (Å)	20–1.70 (1.73–1.70)[a]	20–2.33 (2.37–2.33)
Completeness (%)	98.9 (88.0)	98.6 (96.2)
R_{sym} (%)[b]	5.8 (31.7)	7.8 (22.7)
Phasing Statistics		
Phasing power[c]		
Acentric, anomalous	1.67	
Acentric, isomorphous	1.49	
Centric, isomorphous	2.34	
FOM[d]		
Before density modification	0.36	
After density modification	0.82	
Refinement Statistics		
Number of protein atoms	2437	
Number of heterogeneous atoms	1	
Number of water molecules	301	
R factor	0.2242	
R_{free}	0.2754	
Resolution range (Å)	20–1.70	
Rms deviation from ideality[e]		
Bonds (Å)	0.014	
Angles (°)	2.3	

[a] Numbers in parentheses are for the highest-resolution shell.
[b] $R_{sym} = \Sigma(I - \langle I \rangle)/\Sigma(I)$, where I is the intensity measurement for a given reflection, and $\langle I \rangle$ is the average intensity for multiple measurements of this reflection.
[c] Phasing power equals the heavy-atom structure factor divided by the root-mean-square lack of closure error (statistics from SHARP).
[d] FOM is the figure of merit.
[e] With respect to the Engh and Huber parameter.

i.e., late in biogenesis (Netz et al., 2007). Furthermore, Cia1 has been shown to localize mainly to the nucleus, whereas the other three components are predominantly found in the cytosol. Moreover, the cellular concentration of Cia1 is at least 10-fold higher than that of Cfd1, Nbp35, and Nar1 (Ghaemmaghami et al., 2003). Together, these findings suggest an additional function of Cia1 in the nucleus. In keeping with this notion, the human homolog of yeast Cia1, termed Ciao1, has been demonstrated to interact with the Wilms' tumor suppressor protein, WT1 (Johnstone et al., 1998). WT1 is a zinc-dependent transcription factor that is capable of activating or repressing various cellular genes. Mutations within the WT1 gene have been detected in ~10% of sporadic Wilms' tumors.

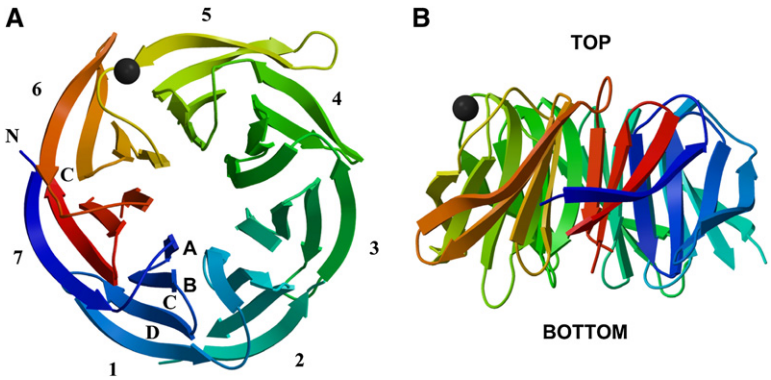

Figure 1. Crystal Structure of *S. cerevisiae* Cia1

(A) A view of the Cia1 structure looking down on "top" of the propeller axis; blades are numbered 1–7. The four antiparallel strands comprising blade 1 are labeled A–D from the central tunnel to the outside of the propeller. The black ball represents the calcium ion bound to the crystallized protein.

(B) The structure rotated by 90°. The figures were prepared with the programs MOLSCRIPT (Kraulis, 1991) and Raster3D (Merritt and Murphy, 1994).

Wilms' tumors, also known as nephroblastomas, mainly affect children. Thus, Ciao1, by interacting with WT1, may function in the regulation of cell growth and differentiation.

Cia1 belongs to the "WD40-repeat" protein family (Smith et al., 1999), and it is predicted to contain seven WD40 repeats. The best-characterized WD40-repeat protein is the Gβ subunit of the heterotrimeric G proteins, including the retinal G protein transducin (Lambright et al., 1996; Sondek et al., 1996; Wall et al., 1995). Therefore, the proteins that contain these WD40 repeats are classified as "transducin-like" or "Gβ-like" to imply that there is some functional similarity between these proteins. However, the known functions of proteins that possess WD40 repeats span a broad spectrum of cellular functions such as vesicular trafficking (Sec13), transcription regulation (Tup1), and cell cycle control (Cdc4). The consensus idea is that the WD40 proteins coordinate the assembly of multiprotein complexes by functioning as a docking site for other proteins. Distinct binding sites for WD40 partner proteins were shown to be located (1) at the central tunnel region on the top face and (2) at one or two of the WD40 blade regions on the top/side face of the WD40 proteins (Ford et al., 1998). One protein specifically interacting with Cia1 in vivo is Nar1, explaining the role of both proteins late in cytosolic Fe/S cluster assembly (Balk et al., 2005; Netz et al., 2007). To gain more detailed insights into Cia1 function in particular and cytosolic Fe/S protein biogenesis in general, the three-dimensional (3D) structure of yeast Cia1 was determined. The 3D structure was used for site-directed mutagenesis to study the functional importance of conserved amino acid residues at the surface of Cia1. We further analyzed the structural and functional similarity of Cia1 and the related human Ciao1 protein by homology modeling and functional complementation studies. The 3D structure of a CIA protein and the biochemical studies provide initial molecular insight into this unique class of eukaryotic WD40 proteins.

RESULTS AND DISCUSSION

Structural Architecture of Cia1 and Comparison to the Gβ Propeller Structure

S. cerevisiae Cia1 was synthesized in *E. coli*, purified to homogeneity, and crystallized (see Experimental Procedures). The 3D structure of Cia1 was determined to 1.7 Å resolution (see Table 1 for details). The Cia1 protein folds into a seven-bladed β propeller with amino acid residues 3–326 (Figure 1). The seven blades are arranged pseudo symmetrically around a central axis. Each blade of the propeller is a β sheet composed of four antiparallel β strands. The blades are numbered 1–7, and, within each blade, the strands are labeled A, B, C, and D from the inside to the outside of the propeller. The loops connecting strands D and A define the "DA loops," and those connecting B and C define the "BC" loops. The "top" face of the propeller is formed by the DA loops, leaving the opposite surface as the "bottom" face.

The seven blades circularize into a propeller arrangement by the juxtaposition of strand C7 and the first D strand at the N terminus, labeled D7. The central channel arising from this circularization is ~12 Å in diameter and is lined mainly by charged residues, namely, Asp21, Arg62, Lys157, His158, Asn255, and Lys302. The channel itself is filled with water molecules. A calcium ion was fitted into a strong electron density region between blades 5 and 6 and made close contacts (<2.6 Å) with the Ser221 residue and four ordered water molecules. The metal-binding site may simply reflect the high concentration (100 mM) of calcium chloride that was present in the crystallization buffer. The nature of the binding site suggests a low affinity; therefore, calcium may not play any physiological role in Cia1 function. This view is further supported by the fact that Ser221 is not conserved in eukaryotic Cia1 proteins (Figure 2).

The amino acid sequence alignment of Cia1 from several different species was used to better understand the structural elements that could be responsible for proper folding and stability (Figure 2). Secondary structure assignments based on the crystal structure are depicted on the top of the alignment. The alignment clearly shows that the highly invariant residues (marked by red boxes) and the conserved substitutions (red residues) are in the structural core of the WD40-repeat domains. The WD40 repeat comprises a 44–60 residue-long sequence that typically contains the GH dipeptide, which is 11–24 residues from the N terminus, and the WD40 dipeptide at the C terminus (Neer et al., 1994). Although the amino acid sequence of the yeast Cia1 contains neither the GH nor the WD40 dipeptide in all blades of the propeller, the

structural integrity is maintained by conserved substitutions in these positions. The length of the sequence between strands B and C from all seven blades is highly conserved, and this loop region contains the highly conserved Asp residue that is present in almost 84% of the repeats. A Glu or Asn residue is conservatively substituted for this Asp in a few species. There is also a high frequency of charged residues, Arg and Glu, located at the end of the strands in the propeller domain, resulting in the formation of ion pairs between neighboring blades.

The overall compact and stable arrangement of the β propeller motif is further provided by hydrogen bonds forming a network between the blades that comprise some of the most conserved residues in the WD40 repeat. This "structural tetrad" or "hydrogen bond network"involving the residues Trp-Thr/Ser-His-Asp has been shown to be a main feature of the crystal structures of the C-terminal domain of Tup1 (Sprague et al., 2000), of Gβ (Sondek et al., 1996), and of other β propeller structures (Cheng et al., 2004). In the Cia1 structure, the hydrogen bond network is formed between Trp in strand C, Ser/Thr in strand B, His in the DA loop, and Asp in the turn between strands B and C.

Although the amino acid sequence comparison between Cia1 and Gβ shows only 16% identity, their 3D structures align remarkably well, with an rmsd of 1.5 Å over 292 Cα atoms, as shown in Figure 3. The individual blades of both proteins align well, and the greatest differences are in the loop regions connecting the strands. In the crystal structure of Cia1, the loop regions consisting of residues Glu88–Thr94 (CD loop), Gly105–Asn108 (DA loop), and Glu305–Lys309 (AB loop) were highly disordered and were absent in the electron density map. Similar gaps have been observed in crystal structures of other propeller proteins, e.g., in Tup1 (Sprague et al., 2000). Furthermore, the Cia1 residues Lys42–Asp45 (CD loop), Lys58 (DA loop), and Glu233 and Asp234 (CD loop) could only be modeled as alanine residues. Therefore, the CD loops are the most flexible, whereas the BC loops are short and less variable in both structures. The exceptions are in the CD loops of blades 4 and 6 that are stabilized by short, tight turns in the Cia1 crystal structure.

An invariant Asp, which is the most conserved residue in all WD40 proteins, stabilizes the BC loops. In the Cia1 structure, this Asp participates in the structural tetrad and forms a hydrogen bond with the protein backbone, thereby forming a tight turn and stabilizing the BC loops as mentioned before. In Gβ, this invariant Asp residue is replaced by Asn, which disturbs the hydrogen bond network in blade 1, but is present in all other blades (2–7). Furthermore, as seen in the superimposition of the Cia1 and Gβ crystal structures shown in Figure 3, the CD loop of blade 5 is considerably longer in Cia1, and the DA loop of blade 2 is much shorter compared to those of Gβ. Furthermore, it can be seen that the Gβ protein has a long N-terminal extension that forms an α helix and interacts with the Gγ subunit in the trimeric G protein complex (Wall et al., 1995). This difference in the loop regions and N-terminal extensions could have implications for the different functions and interaction partners of these two proteins.

Site-Directed Mutagenesis and Implications for Protein-Protein Interactions

The WD40-repeat propeller structures provide a stable platform that may form complexes with partner proteins for functional interaction (Smith et al., 1999). Thus far, Cia1 has been reported to functionally interact with the CIA protein Nar1 (Balk et al., 2005). Other potential interactions have been suggested by systematic studies (Ho et al., 2002; Krogan et al., 2006). Furthermore, the occurrence of a *CFD1-CIA1* fusion gene in *S. pombe* may indicate an interaction with the P loop NTPase Cfd1, even though this may be weak or transient (Balk et al., 2005). It has been shown that preferential binding surfaces for proteins are characterized as having high solvent accessibility and a high degree of conformational flexibility in conserved regions. Mapping of the conserved residues on the surface of Cia1 was performed from CLUSTAL multisequence alignment (Thompson et al., 1994) of 67 Cia1 and Ciao1 proteins and the program ConSurf (Landau et al., 2005) (Figure 4). It becomes evident that the conserved patches of residues are located mainly on the "top" of the propeller, around the central tunnel, and on one side, mainly comprising blades 2 and 3 and almost all of the DA and BC loops. In contrast, there is only low conservation observed on the "bottom" surface.

To initiate the functional analysis of the Cia1 structure, we investigated the role of surface-exposed residues in Cia1 function by using a structure-based site-directed mutagenesis approach. Conserved residues within the loop regions of Cia1 exhibiting high solvent accessibility were exchanged, and, in most cases, the charge of selected residues was reversed (Figures 2 and 5A). Our mutational strategy aimed at keeping the overall solubility of the protein high. Furthermore, in order to avoid major structural changes, we did not exchange any residues in the structure-forming core of the seven WD40 propeller blades. The consequences of the amino acid exchanges were tested by complementing Cia1-depleted Gal-CIA1 cells with plasmids encoding mutated *CIA1*. These cells contain the galactose-inducible and glucose-repressible *GAL1-10* promoter in front of *CIA1*, allowing depletion of Cia1 by growth on glucose-containing media (Balk et al., 2005). As a result, these cells show a characteristic growth defect that can be fully rescued by a plasmid-borne *CIA1* gene. Most mutant *CIA1* genes were able to restore wild-type growth of Cia1-depleted Gal-CIA1 cells, indicating that the mutated residues play no critical role in Cia1 function (Figure 5A). This makes it unlikely that these residues are involved in establishing direct contacts to partner proteins. In contrast, one mutant (R127E) elicited only a weak reversal of the growth defect. This result suggested that Arg127 is important for the function of Cia1. To further examine the biochemical consequences of the mutation, the enzyme activities of some reporter proteins in the cytosol and mitochondria were measured. The activity of

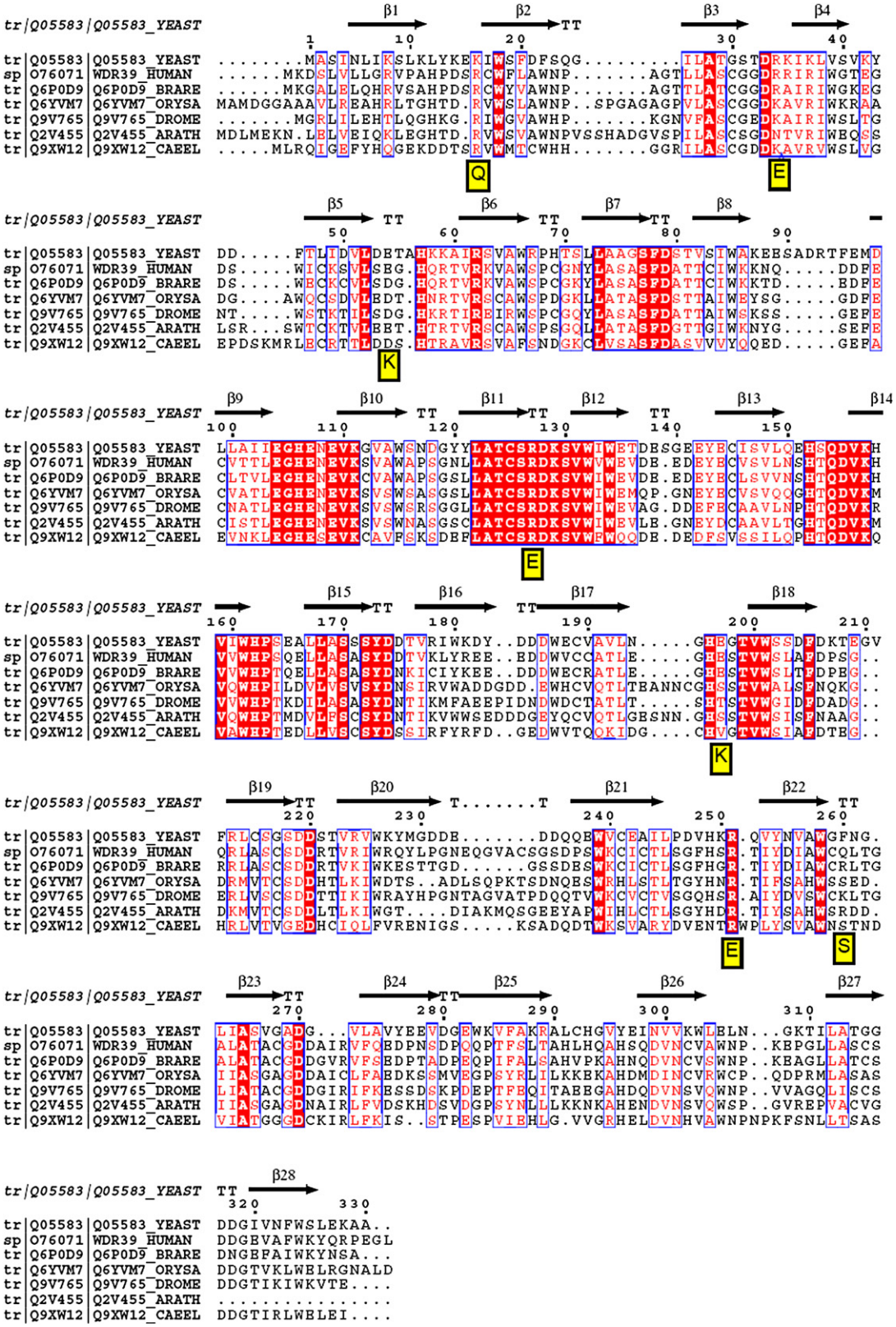

Figure 2. Structure-Based Sequence Alignment of Cia1 Proteins

An alignment of the amino acid sequences of Cia1 protein from *S. cerevisiae, Homo sapiens*, *Danio rerio*, *Oryza sativa*, *Drosophila melanogaster*, *Arabidopsis thaliana*, and *Caenorhabditis elegans* with the program CLUSTAL W (Thompson et al., 1994). Invariant residues are shown in red boxes,

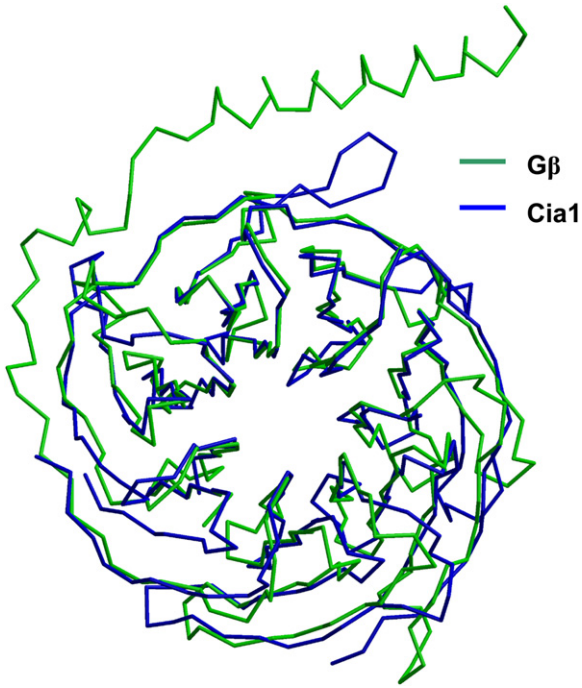

Figure 3. Comparison of the 3D Structures of Cia1 and Gβ
Superposition of the Cα coordinates of Gβ (PDB code: 1TBG) and the crystal structure coordinates of yeast Cia1. The superposition was computed by using the least-squares algorithm in the program O (Jones et al., 1991).

the cytosolic Fe/S protein Leu1 was decreased to 28% in Cia1-depleted Gal-CIA1 cells after 36 hr of growth on glucose-containing media, whereas the activity of the mitochondrial Fe/S proteins aconitase (Aco1) and succinate dehydrogenase (SDH) remained at wild-type levels (Figures 5B and 5C). The activities of two control proteins, alcohol dehydrogenase (cytosol) and citrate synthase (mitochondrion), that do not carry Fe/S clusters remained unchanged. Quantitative immunostaining analysis showed that the protein amount of Leu1 in the mutant R127E was slightly reduced, but far less so than the enzyme activity. The protein levels of the other examined enzymes did not change significantly. We conclude that mutation of Arg127 causes a specific defect of Cia1 and thus is critical to its function.

To further examine the effect of this R127E mutation, we performed a radiolabeling experiment to follow the de novo assembly of Fe/S proteins (Kispal et al., 1999). In this assay, cells are labeled with ^{55}Fe, a cell extract is prepared, the Fe/S proteins of interest are immunoprecipitated, and bound ^{55}Fe is estimated as a measure of Fe/S cluster incorporation by scintillation counting. The ^{55}Fe incorporation into Leu1 was significantly decreased by 35% in the R127E mutant, while no changes in the maturation of Aco1 were observed compared to wild-type control, thus supporting the enzyme activity measurements of Leu1 and Aco1 (Figure 5D). In summary, these results indicate that the charge inversion in the R127E mutant led to a functional impairment of Cia1, even though the mutated protein retained some residual activity. Thus, Arg127 plays an important, but not essential, role for Cia1 function.

Structural and Functional Similarity between Yeast Cia1 and Its Human Homolog Ciao1

The human homolog of Cia1, termed Ciao1, has been identified as a protein that specifically interacts with the Wilms' tumor suppressor protein, WT1, both in vitro and in vivo (Johnstone et al., 1998). Since WT1 is a zinc finger-containing transcription factor, it seems possible that Ciao1 performs a role in activating or repressing transcription. Given its medical importance, it was of interest to structurally and functionally compare the yeast and human Cia1 proteins. The amino acid sequences of the yeast and human Cia1 proteins show 42% identity and 64% similarity over their entire lengths. This fairly high sequence conservation is reflected in a high structural similarity, which was estimated by homology modeling for human Ciao1 on the basis of the crystal structure coordinates of yeast Cia1 (Schwede et al., 2003). The Ciao1 structural model shows a well-conserved arrangement of the seven-bladed β propeller, especially in the cores of the individual blades (not shown).

The high structural similarity raised the question of whether human Ciao1 can replace yeast Cia1 in its essential functions in cell growth and in cytosolic Fe/S protein assembly. We inserted the cDNA of the human gene into a yeast expression vector and transformed this vector into Gal-CIA1 cells. Human Ciao1 fully restored the growth defect observed upon depletion of the endogenous yeast Cia1 on glucose-containing medium (Figure 6A). No difference in growth was seen on galactose-containing medium, indicating that (over-) production of the human protein in yeast had no detrimental effects. We next measured the functional consequences of Ciao1 expression in yeast on cytosolic Fe/S protein maturation. To this end, extracts were prepared from Cia1-depleted Gal-CIA1 cells expressing plasmid-borne yeast *CIA1* or human *CIAO1*. The enzyme activity of the cytosolic Fe/S protein Leu1 was measured. Both yeast Cia1 and human Ciao1 proteins were able to restore the low Leu1 enzyme activity in Cia1-depleted Gal-CIA1 cells to a similar extent (Figure 6B). The Leu1 protein levels hardly changed in these experiments (Figure 6C). These data clearly demonstrate that human Ciao1 can replace its yeast homolog in cytosolic Fe/S protein maturation. The structural and

conserved substitutions are shown as red characters, and gaps are indicated as dots. The numbering corresponds to the sequence of Cia1 from *S. cerevisiae*. Secondary structural elements were calculated by using DSSP (Kabsch and Sander, 1983) and are represented on top of the alignment. The figure was prepared with ESPript (Gouet et al., 1999). Residues introduced into *S. cerevisiae* Cia1 by site-directed mutagenesis are indicated in yellow below the alignment.

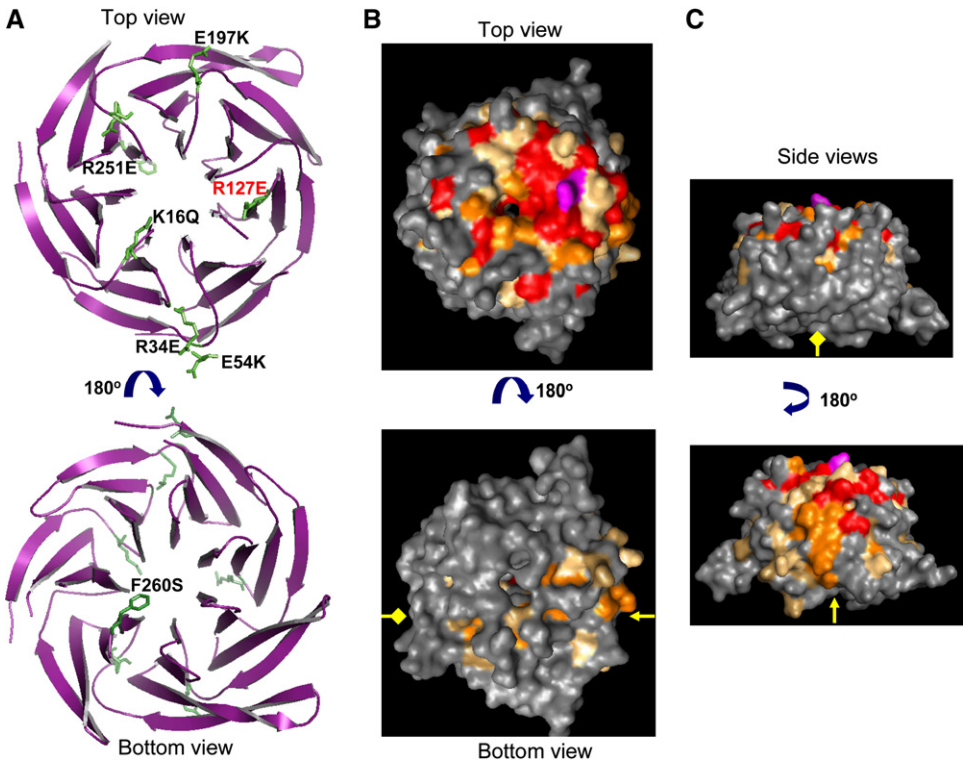

Figure 4. Amino Acid Sequence Conservation at the Surface of Cia1

(A) Location of the residues exchanged by site-directed mutagenesis (see Figure 2) from a top view looking down the central propeller axis and a bottom view obtained by rotation of 180°.

(B) Representation of the conservation of amino acid residues in Cia1 from top and bottom views. The degree of conservation is indicated by the intensity of the red color. The position of the crucial residue R127 is highlighted in purple. Amino acid sequences (67 in total) of Cia1 homologs were collected from various databases by blastp and tblastn searches. After CLUSTAL W alignment (Thompson et al., 1994), the degree of conservation was calculated by using the program ConSurf (Landau et al., 2005). Red, orange, and light-orange colors correspond to residues with a conservation score above the 9th, between the 9th and 8th, and between the 8th and 7th decile, respectively.

(C) Same as in (B), but for the side views. The yellow markers in (B) and (C) indicate the respective sides of the Cia1 structure. The figure was prepared by using PyMol (http://www.pymol.org) (DeLano, 2002).

functional similarity of the two Cia1 homologs makes it likely that Ciao1 also performs a role in Fe/S protein maturation in human cells. To our knowledge, this represents the first example of a functional replacement of a yeast CIA protein by its mammalian counterpart. The finding suggests a functional conservation of the CIA machinery in eukaryotes. Similarly, members of the mammalian Fe/S cluster assembly and export machineries have been reported to functionally replace the yeast Fe/S cluster proteins, indicating a general functional conservation of Fe/S protein biogenesis in both lower and higher eukaryotes (Bekri et al., 2000; Biederbick et al., 2006; Gerber et al., 2004; Lange et al., 2001; Wilson and Roof, 1997; Wingert et al., 2005).

Based on both these and earlier findings (Johnstone et al., 1998), it seems possible that Ciao1 performs a dual function, one in Fe/S protein maturation and another one in the regulation of transcription. The possibility of depleting the cellular concentration of human proteins by the RNAi technology will allow for the testing of these ideas in human cell culture. Whether yeast Cia1 performs a second function in transcription is unclear at present. Its high concentration and its abundance in the nucleus compared to the fairly low levels of Cfd1, Nbp35, and Nar1 in the nucleus (Balk et al., 2005) may fit with the idea that the nuclear fraction of Cia1 participates in a process other than Fe/S protein maturation. Direct studies have to verify this potential transcriptional role of Cia1 in yeast.

To our knowledge, our studies provide the first structural insight into a component of the CIA machinery. Cia1, as a member of the large WD40-repeat protein family, may use its doughnut-shaped structure to facilitate protein interactions between other members of the CIA machinery. Thus far, only one member, Nar1, has been found to interact with Cia1. However, systematic interaction studies indicate that there are a number of other proteins that may represent potential functional partners of Cia1 (Ho et al., 2002; Krogan et al., 2006). The structural and functional data provided in this study will be invaluable for identifying additional specific interaction partners of Cia1 and for mapping their interaction sites. Since our data suggest a general conservation of the CIA proteins in eukaryotes, our data may be of general importance for all eukaryotes.

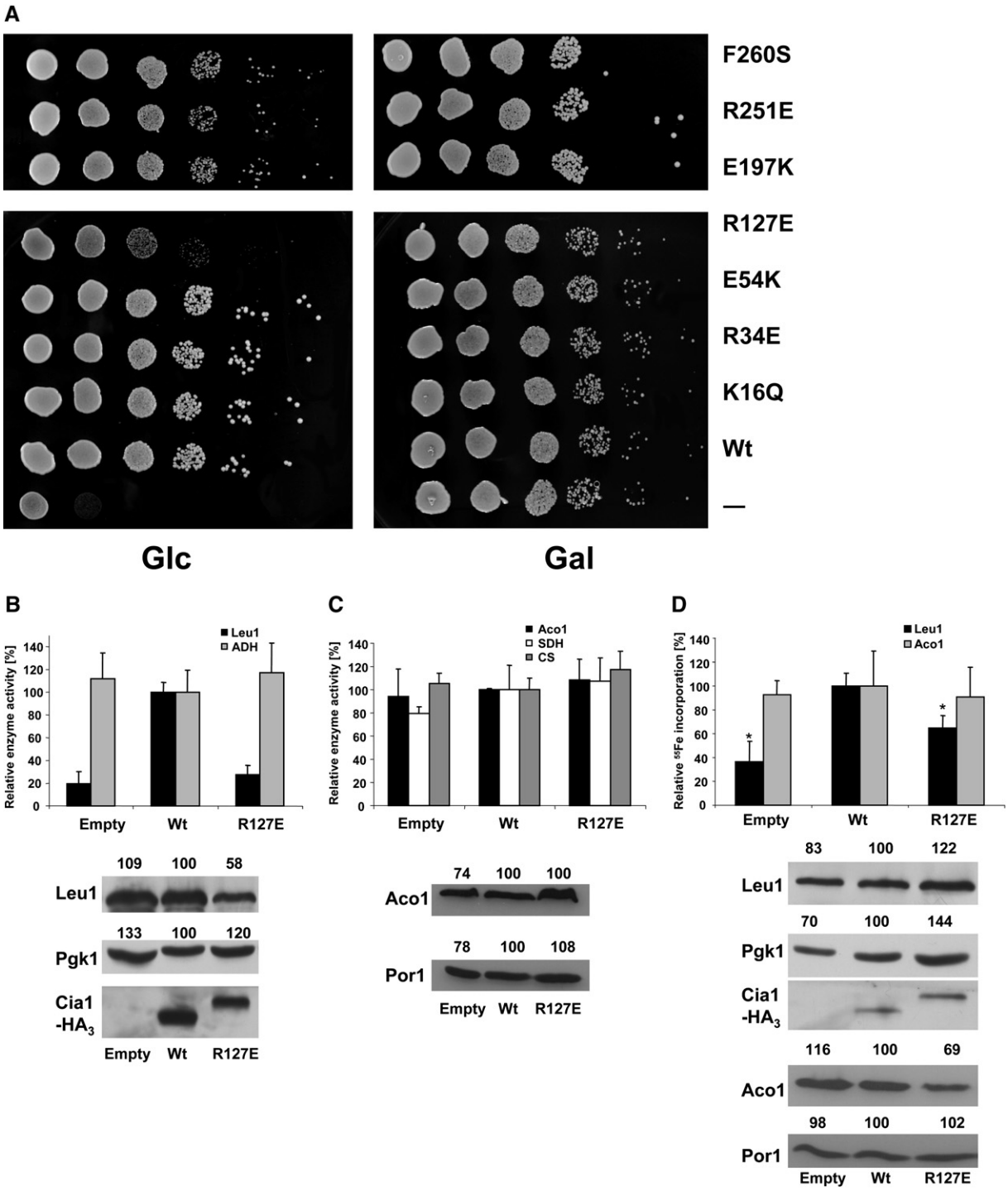

Figure 5. Site-Directed Mutagenesis Reveals the Importance of R127 for Cia1 Function

(A) Growth phenotype of *CIA1* point mutations. Gal-CIA1 cells carrying a regulatable *CIA1* gene were transformed with plasmid p416 containing either no gene (–), the wild-type HA_3-tagged *CIA1* gene (Wt), or the corresponding indicated point mutations. Cells were grown for 7 days on agar plates containing minimal media with galactose (Gal) or glucose (Glc). Downregulated cells were washed with water, and 10-fold dilutions with a starting OD_{600} of 1.5 were spotted on fresh agar plates.

(B) Mutation of residue R127 of Cia1 leads to decreased activity of the cytosolic Fe/S protein Leu1. Gal-CIA1 cells were transformed with the vector p416 carrying either no gene, the wild-type *CIA1-HA*$_3$, or the mutated *R127E CIA1-HA*$_3$. These cells were grown on minimal medium containing galactose or glucose for 36 hr. Cells were harvested and lysed, and the extracts were used for measurement of the enzyme activities of the cytosolic enzymes isopropylmalate isomerase (Leu1) and alcohol dehydrogenase (ADH). The relative values obtained for cells grown in the presence of glucose

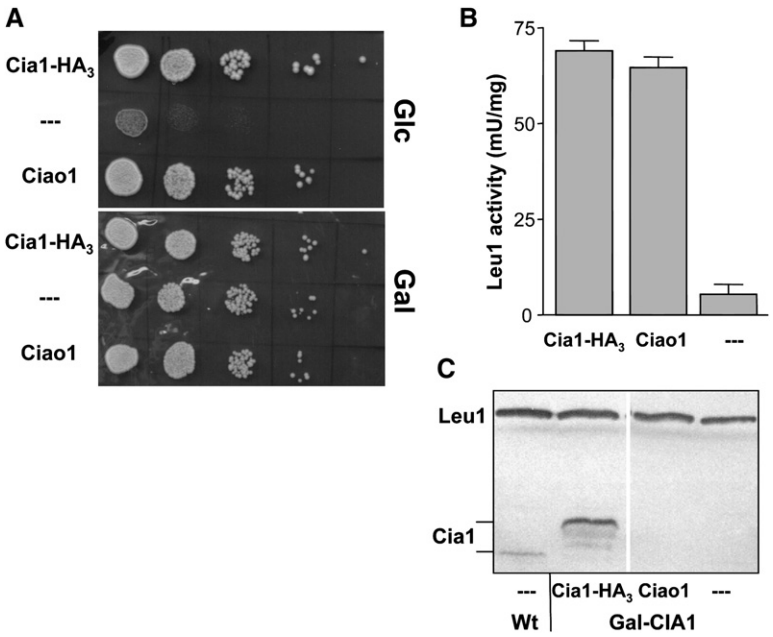

Figure 6. Human Ciao1 Can Functionally Replace Yeast Cia1 in Fe/S Protein Maturation

(A) Gal-CIA1 cells were transformed with the yeast expression vector p316 containing no gene (–), the cDNA of human *CIAO1*, or the yeast *CIA1-HA$_3$* fusion gene. Cells were grown twice for 2 days at 30°C on agar plates containing rich medium supplemented with galactose (Gal) or glucose (Glc). 10-fold serial dilutions were spotted.

(B) Gal-CIA1 cells from (A) were grown in glucose-containing minimal media and were used to measure the enzyme activity of Leu1 as described in Figure 5B. Error bars represent the standard error of the mean.

(C) Cell extracts from (B) were used for immunostaining of Leu1 and Cia1 with specific antisera. Endogenous Cia1 in extracts from wild-type (Wt) cells is shown as a control and is smaller than its HA$_3$-tagged version.

EXPERIMENTAL PROCEDURES

Cloning and Expression of CIA1 and Protein Purification

The *CIA1* gene was isolated from genomic DNA of the wild-type yeast strain W303 by using PCR and was cloned into the multiple cloning site I of pRSFDuet-1 and pCOLADuet-1 (both from Novagen) for heterologous expression in *E. coli*. For insertion, the EcoRI and HindIII restriction sites were used in order to fuse an N-terminal hexahistidine tag sequence (encoded by the vector) to Cia1. DNA sequencing detected a sequence variation at position 923 in our yeast strain background compared to the published *CIA1* DNA sequence. The base substitution G923A apparently did not affect the function of the protein.

Full-length Cia1 carrying an N-terminal His tag was produced in *E. coli* B21 (DE3) by using pRSFDuet-1. Cells were disrupted in NTA purification buffer (QIAGEN) by one passage (15,000 psi, 4°C) through a homogenizer (Avestin). After centrifugation (100,000 × g, 45 min, 4°C), purification was performed by Ni-NTA agarose chromatography according to the manufacturer's instructions (QIAGEN). The eluate was concentrated by using a 10,000 MWCO concentrator (Millipore) and was subjected to gel-filtration chromatography on a 16 × 60 cm Sephacryl S300 column (Amersham). Fresh preparations were used for crystallization studies. Purity and homogeneity was assessed by analytical size-exclusion chromatography and SDS-PAGE. Cia1 was labeled with selenomethionine via metabolic inhibition (Van Duyne et al., 1993). In brief, pCOLADuet-1 was used as an expression vector, since better growth and higher expression of *CIA1* was obtained. The cells of a 5 ml overnight preculture in LB medium were pelleted, resuspended in 1 ml prewarmed M9 medium, and added to 1 l of the same medium. When the culture reached an OD of 0.5, a solution of amino acids (100 mg L-lysine, 100 mg L-phenylalanine, 100 mg L-threonine, 50 mg L-leucine, 50 mg L-valine, and 50 mg L-selenomethionine per 1 l M9 medium) was added, and the mixture was incubated for 15 min. Expression was induced by the addition of 1 mM IPTG (Roth), followed by overnight incubation at 30°C. Purification of selenomethionine-labeled, His-tagged Cia1 was performed as described above, with the minor modification that the buffer used for gel filtration was degassed with argon before use and contained 1 mM DTT.

Crystallization and Data Collection

The purified protein was concentrated to 12 mg/ml and crystallized by using the hanging-drop vapor-diffusion method against a reservoir containing 22% PEG 4000, 20 mM Tris-HCl (pH 8.5), and 100 mM $CaCl_2$. For data collection, a single crystal was harvested directly from the mother liquor and flash frozen in a liquid nitrogen stream at 100 K. No cryoprotectant solution was added, as the protein storage buffer contained 10% glycerol. A native data set from this single crystal was collected at the Swiss Light Source, beamline PX06, on a MAR CCD detector to a resolution of 1.70 Å. Crystals of the selenomethionine-labeled protein were grown in the same way as the native protein, and a peak data set close to the absorption edge of the selenium atom was collected at the EMBL Hamburg beamline X31. These crystals diffracted to a resolution of 2.33 Å. All data were indexed, integrated, and

and galactose were plotted. The bottom part shows immunostains for Leu1, phosphoglycerate kinase (Pgk1, cytosol), and the HA$_3$ tag of Cia1. The relative amounts of protein were estimated by densitometry and are indicated above the blots. The mutated Cia1 R127E showed a diminished mobility on SDS-PAGE. This is probably due to the charge reversion.

(C) The Cia1 R127 mutation has no effect on mitochondrial functions. Mitochondria were isolated from cells described in (B). The relative activities of the mitochondrial enzymes aconitase (Aco1), succinate dehydrogenase (SDH), and citrate synthase (CS) were estimated. Immunoblot analyses and quantitation were done for Aco1 and porin (Por1) as loading controls.

(D) A specific defect in the de novo assembly of cytosolic Leu1 Fe/S protein upon mutation of R127 in Cia1. Gal-CIA1 cells from (B) were grown in glucose-containing minimal medium for 24 hr. Growth was continued for 12 hr in iron-poor minimal medium in the presence of glucose, and cells were then radiolabeled with ^{55}Fe for 2 hr. An extract was prepared, and Leu1 or Aco1 was immunoprecipitated with specific antisera. Scintillation counting was used for quantification of ^{55}Fe incorporation and immunoblot analyses for assessing protein levels. All experiments were repeated between three and eight times.

Error bars represent the standard error of the mean; the asterisk indicates p > 95%.

scaled by using the HKL suite of programs, DENZO, and SCALEPACK (Otwinowski and Minor, 1997). The space group was determined to be $P2_12_12_1$ based on the unit cell dimensions a = 35.699, b = 71.450, c = 131.169 Å, $\alpha = \beta = \gamma = 90^\circ$ and the systematic absence of axial reflections. The asymmetric unit contains one molecule with a molecular mass of 37,200 Da, resulting in an apparent V_m of 2.2 $Å^3$/Da and a solvent content of 42.6% (Matthews, 1968). Data collection and processing statistics are listed in Table 1.

Structure Determination and Refinement

The crystal structure of the Cia1 protein was determined by the single-wavelength anomalous diffraction (SAD) technique. Transformation from intensity data to structure factor amplitudes and anomalous differences was done with the program TRUNCATE in the CCP4 suite of programs (CCP4, 1994). Attempts to solve the structure by using the molecular replacement method with several existing seven-bladed β propeller structures in the Protein Data Bank as models did not result in a clear solution. Hence, the selenomethionine-labeled protein was prepared as described above, and a data set was collected close to the absorption edge of the selenium atom. SHELXD (Sheldrick and Schneider, 1997) was used to locate the selenium atoms and clearly showed two selenium atom positions. These positions were then refined, and phases were computed by using the program SHARP (De la Fortelle and Bricogne, 1997). Further improvement of phases by using solvent flattening with the program DM assuming a solvent content of 50% revealed an electron density map that was partly interpretable. The structure solution was not straightforward due to a combination of nonisomorphism between the native and selenomethionine-labeled crystals and also to the low selenium content in the crystals (3 methionines in 330 residues and only 2 selenium atoms were incorporated into the protein). Although the resolution of the native data set extended to 1.7 Å and was 98.9% complete, automatic model building with the program ARP/WARP (Morris et al., 2003) was not successful due to lack of good phase information. About one-third of the molecule could be traced manually by visual inspection of the $F_o - F_c$ and $2F_o - F_c$ maps with the program O (Jones et al., 1991). This partial model was then put into ARP/WARP, and ~90% of the model was built automatically. Few residues in the loops were further manually built and put into ARP/WARP to complete the final model. During the final stages of the model building, water molecules were added by using ARP/WARP. A final restrained refinement with Refmac5 by using TLS parameters brought the R factor to 22.4% and R_{free} to 27.5%. The final model consists of 308 amino acid residues, 301 water molecules, and a calcium ion. No electron density was observed for the first two N-terminal (Met and Ala) and the last four C-terminal amino acid residues. Furthermore, the loop regions consisting of residues Glu88–Thr94, Gly105–Asn108, and Glu305–Lys309 were highly disordered and absent in the electron density map. Furthermore, the residues Lys42–Asp45, Lys58, Glu233, and Asp234 could only be modeled as alanine residues. The stereochemical quality of the structure was examined with PROCHECK (Laskowski et al., 1993) and WHAT-CHECK (Hooft et al., 1996). A total of 84.4% residues occupy the most favored regions, and 15.6% occupy the additionally allowed regions of the Ramachandran map; no residue occupied the disallowed region of the map. The refinement statistics and quality of the final model are summarized in Table 1.

Yeast Strains, Cell Growth, Plasmids, and Site-Directed Mutagenesis

The previously described yeast strain Gal-CIA1 (Balk et al., 2005) was grown at 30°C in rich (YP) or minimal (SC) media containing the required carbon sources at a concentration of 2% (w/v) (Sherman, 1991). The plasmid p416 (Mumberg et al., 1995) containing the *MET25* promoter in front of a triple HA (hemagglutinin)-tagged *CIA1* gene or its mutated versions was used. Mutations were introduced into *CIA1* by PCR with appropriate complementary mutagenic primers with *CIA1-HA*$_3$ in plasmid p416 as a template (Balk et al., 2005). After digestion of the parental DNA template with the DpnI restriction endonuclease (NEB), the PCR-generated plasmid was directly transformed into *E. coli* DH5α (Novagen) (Costa et al., 1996). The coding sequence of human *CIAO1* was amplified from its cDNA (kindly provided by Ricky W. Johnstone [Johnstone et al., 1998]) by PCR, and it was cloned into the yeast plasmid p416 to obtain p416-CIAO1. All constructs were verified by DNA sequencing.

Miscellaneous Methods

The following published methods were used: manipulation of DNA and PCR (Sambrook and Russell, 2001); transformation of yeast cells (Gietz et al., 1992); preparation of yeast mitochondria (Diekert et al., 2001); determination of the enzyme activities of alcohol dehydrogenase (EC 1.1.1.1), isopropylmalate isomerase (EC 4.2.1.33), succinate dehydrogenase (EC 1.3.5.1), aconitase (EC 4.2.1.3), and citrate synthase (EC 2.3.3.1) (Kispal et al., 1999; Mühlenhoff et al., 2002); radiolabeling of the Fe/S reporter proteins with ^{55}Fe, cell lysis, and quantification of ^{55}Fe/S protein assembly by immunoprecipitation and scintillation counting (Kispal et al., 1999; Mühlenhoff et al., 2002).

ACKNOWLEDGMENTS

We thank Dr. R.W. Johnstone for providing the cDNA of Ciao1 and Dr. S. Panjikar (EMBL, Hamburg) for valuable discussion. Our work was generously supported by the Max-Planck-Gesellschaft, Deutsche Forschungsgemeinschaft (SFB 593 and TR1, Gottfried-Wilhelm Leibniz program, and GRK 1216), and Fonds der chemischen Industrie.

Received: June 12, 2007
Revised: August 2, 2007
Accepted: August 9, 2007
Published: October 16, 2007

REFERENCES

Balk, J., Pierik, A.J., Aguilar Netz, D., Mühlenhoff, U., and Lill, R. (2004). The hydrogenase-like Nar1p is essential for maturation of cytosolic and nuclear iron-sulphur proteins. EMBO J. *23*, 2105–2115.

Balk, J., Aguilar Netz, D.J., Tepper, K., Pierik, A.J., and Lill, R. (2005). The essential WD40 protein Cia1 is involved in a late step of cytosolic and nuclear iron-sulfur protein assembly. Mol. Cell. Biol. *25*, 10833–10841.

Beinert, H., Holm, R.H., and Münck, E. (1997). Iron-sulfur clusters: Nature's modular, multipurpose structures. Science *277*, 653–659.

Bekri, S., Kispal, G., Lange, H., Fitzsimons, E., Tolmie, J., Lill, R., and Bishop, D.F. (2000). Human ABC7 transporter: gene structure and mutation causing X-linked sideroblastic anemia with ataxia (XLSA/A) with disruption of cytosolic iron-sulfur protein maturation. Blood *96*, 3256–3264.

Biederbick, A., Stehling, O., Rösser, R., Niggemeyer, B., Nakai, Y., Elsässer, H.P., and Lill, R. (2006). Role of human mitochondrial Nfs1 in cytosolic iron-sulfur protein biogenesis and iron regulation. Mol. Cell. Biol. *26*, 5675–5687.

CCP4 (Collaborative Computational Project, Number 4) (1994). The CCP4 suite: programs for protein crystallography. Acta Crystallogr. D Biol. Crystallogr. *50*, 760–763.

Cheng, Z., Liu, Y., Wang, C., Parker, R., and Song, H. (2004). Crystal structure of Ski8p, a WD-repeat protein with dual roles in mRNA metabolism and meiotic recombination. Protein Sci. *13*, 2673–2684.

Costa, G.L., Bauer, J.C., McGowan, B., Angert, M., and Weiner, M.P. (1996). Site-directed mutagenesis using a rapid PCR-based method. Methods Mol. Biol. *57*, 239–248.

De la Fortelle, E., and Bricogne, G. (1997). Maximum-likelihood heavy-atom parameter refinement for multiple isomorphous replacement and multiwavelength anomalous diffraction methods. Methods Enzymol. *276*, 472–494.

DeLano, W.L. (2002). The PyMOL Molecular Graphics System (http://www.pymol.org).

Diekert, K., deKroon, A.I.P.M., Kispal, G., and Lill, R. (2001). Isolation and sub-fractionation of mitochondria from the yeast *Saccharomyces cerevisiae*. Methods Cell Biol. *65*, 37–51.

Dong, J., Lai, R., Nielsen, K., Fekete, C.A., Qiu, H., and Hinnebusch, A.G. (2004). The essential ATP-binding cassette protein RLI1 functions in translation by promoting preinitiation complex assembly. J. Biol. Chem. *279*, 42157–42168.

Ford, C.E., Skiba, N.P., Bae, H., Daaka, Y., Reuveny, E., Shekter, L.R., Rosal, R., Weng, G., Yang, C.S., Iyengar, R., et al. (1998). Molecular basis for interactions of G protein βγ subunits with effectors. Science *280*, 1271–1274.

Gerber, J., Neumann, K., Prohl, C., Mühlenhoff, U., and Lill, R. (2004). The yeast scaffold proteins Isu1p and Isu2p are required inside mitochondria for maturation of cytosolic Fe/S proteins. Mol. Cell. Biol. *24*, 4848–4857.

Ghaemmaghami, S., Huh, W.K., Bower, K., Howson, R.W., Belle, A., Dephoure, N., O'Shea, E.K., and Weissman, J.S. (2003). Global analysis of protein expression in yeast. Nature *425*, 737–741.

Gietz, D., St. Jean, A., Woods, R.A., and Schiestl, R.H. (1992). Improved method for high efficiency transformation of intact yeast cells. Nucleic Acids Res. *20*, 1425.

Gouet, P., Courcelle, E., Stuart, D.I., and Metoz, F. (1999). ESPript: analysis of multiple sequence alignments in PostScript. Bioinformatics *15*, 305–308.

Hausmann, A., Aguilar Netz, D.J., Balk, J., Pierik, A.J., Mühlenhoff, U., and Lill, R. (2005). The eukaryotic P-loop NTPase Nbp35: an essential component of the cytosolic and nuclear iron-sulfur protein assembly machinery. Proc. Natl. Acad. Sci. USA *102*, 3266–3271.

Ho, Y., Gruhler, A., Heilbut, A., Bader, G.D., Moore, L., Adams, S.L., Millar, A., Taylor, P., Bennett, K., Boutilier, K., et al. (2002). Systematic identification of protein complexes in *Saccharomyces cerevisiae* by mass spectrometry. Nature *415*, 180–183.

Hooft, R.W., Vriend, G., Sander, C., and Abola, E.E. (1996). Errors in protein structures. Nature *381*, 272.

Johnstone, R.W., Wang, J., Tommerup, N., Vissing, H., Roberts, T., and Shi, Y. (1998). Ciao1 is a novel WD40 protein that interacts with the tumor suppressor protein WT1. J. Biol. Chem. *273*, 10880–10887.

Jones, T.A., Zou, J.Y., Cowan, S.W., and Kjeldgaard, M. (1991). Improved methods for building protein models in electron density maps and the location of errors in these models. Acta Crystallogr. A *47*, 110–119.

Kabsch, W., and Sander, C. (1983). Dictionary of protein secondary structure: pattern recognition of hydrogen-bonded and geometrical features. Biopolymers *22*, 2577–2637.

Kispal, G., Csere, P., Prohl, C., and Lill, R. (1999). The mitochondrial proteins Atm1p and Nfs1p are required for biogenesis of cytosolic Fe/S proteins. EMBO J. *18*, 3981–3989.

Kispal, G., Sipos, K., Lange, H., Fekete, Z., Bedekovics, T., Janaky, T., Bassler, J., Aguilar Netz, D.J., Balk, J., Rotte, C., et al. (2005). Biogenesis of cytosolic ribosomes requires the essential iron-sulphur protein Rli1p and mitochondria. EMBO J. *24*, 589–598.

Kraulis, P.J. (1991). MOLSCRIPT: a program to produce both detailed and schematic plots of protein structures. J. Appl. Cryst. *24*, 946–950.

Krogan, N.J., Cagney, G., Yu, H., Zhong, G., Guo, X., Ignatchenko, A., Li, J., Pu, S., Datta, N., Tikuisis, A.P., et al. (2006). Global landscape of protein complexes in the yeast *Saccharomyces cerevisiae*. Nature *440*, 637–643.

Lambright, D.G., Sondek, J., Bohm, A., Skiba, N.P., Hamm, H.E., and Sigler, P.B. (1996). The 2.0 Å crystal structure of a heterotrimeric G protein. Nature *379*, 311–319.

Landau, M., Mayrose, I., Rosenberg, Y., Glaser, F., Martz, E., Pupko, T., and Ben-Tal, N. (2005). ConSurf 2005: the projection of evolutionary conservation scores of residues on protein structures. Nucleic Acids Res. *33*, W299–W302.

Lange, H., Lisowsky, T., Gerber, J., Mühlenhoff, U., Kispal, G., and Lill, R. (2001). An essential function of the mitochondrial sulfhydryl oxidase Erv1p/ALR in the maturation of cytosolic Fe/S proteins. EMBO Rep. *2*, 715–720.

Laskowski, R.A., Moss, D.S., and Thornton, J.M. (1993). Main-chain bond lengths and bond angles in protein structures. J. Mol. Biol. *231*, 1049–1067.

Lill, R., and Mühlenhoff, U. (2005). Iron-sulfur protein biogenesis in eukaryotes. Trends Biochem. Sci. *30*, 133–141.

Lill, R., and Mühlenhoff, U. (2006). Iron-sulfur protein biogenesis in eukaryotes: components and mechanisms. Annu. Rev. Cell Dev. Biol. *22*, 457–486.

Matthews, B.W. (1968). Solvent content of protein crystals. J. Mol. Biol. *33*, 491–497.

Merritt, E.A., and Murphy, M.E. (1994). Raster3D Version 2.0. A program for photorealistic molecular graphics. Acta Crystallogr. D Biol. Crystallogr. *50*, 869–873.

Morris, R.J., Perrakis, A., and Lamzin, V.S. (2003). ARP/wARP and automatic interpretation of protein electron density maps. Methods Enzymol. *374*, 229–244.

Mühlenhoff, U., Richhardt, N., Ristow, M., Kispal, G., and Lill, R. (2002). The yeast frataxin homologue Yfh1p plays a specific role in the maturation of cellular Fe/S proteins. Hum. Mol. Genet. *11*, 2025–2036.

Mumberg, D., Müller, R., and Funk, M. (1995). Yeast vectors for controlled expression of heterologous proteins in different genetic backgrounds. Gene *156*, 119–122.

Neer, E.J., Schmidt, C.J., Nambudripad, R., and Smith, T.F. (1994). The ancient regulatory-protein family of WD-repeat proteins. Nature *371*, 297–300.

Netz, D.J.A., Pierik, A.J., Stümpfig, M., Mühlenhoff, U., and Lill, R. (2007). The Cfd1–Nbp35 complex acts as a scaffold for iron-sulfur protein assembly in the yeast cytosol. Nat. Chem. Biol. *3*, 278–286.

Otwinowski, Z., and Minor, W. (1997). Processing of X-ray diffraction data collected in oscillation mode. Methods Enzymol. *276*, 307–326.

Radford, S.J., Goley, E., Baxter, K., McMahan, S., and Sekelsky, J. (2005). *Drosophila* ERCC1 is required for a subset of MEI-9-dependent meiotic crossovers. Genetics *170*, 1737–1745.

Rouault, T.A., and Tong, W.H. (2005). Iron-sulphur cluster biogenesis and mitochondrial iron homeostasis. Nat. Rev. Mol. Cell Biol. *6*, 345–351.

Roy, A., Solodovnikova, N., Nicholson, T., Antholine, W., and Walden, W.E. (2003). A novel eukaryotic factor for cytosolic Fe-S cluster assembly. EMBO J. *22*, 4826–4835.

Sambrook, J., and Russell, D.W. (2001). Molecular Cloning: A Laboratory Manual, Third Edition (Cold Spring Harbor, NY: Cold Spring Harbor Laboratory Press).

Schwede, T., Kopp, J., Guex, N., and Peitsch, M.C. (2003). SWISS-MODEL: an automated protein homology-modeling server. Nucleic Acids Res. *31*, 3381–3385.

Sheldrick, G., and Schneider, T. (1997). SHELXL: high resolution refinement. Methods Enzymol. *277*, 319–343.

Sherman, F. (1991). Getting started with yeast. Methods Enzymol. *194*, 3–21.

Smith, T.F., Gaitatzes, C., Saxena, K., and Neer, E.J. (1999). The WD repeat: a common architecture for diverse functions. Trends Biochem. Sci. *24*, 181–185.

Sondek, J., Bohm, A., Lambright, D.G., Hamm, H.E., and Sigler, P.B. (1996). Crystal structure of a G-protein βγ dimer at 2.1 Å resolution. Nature *379*, 369–374.

Sprague, E.R., Redd, M.J., Johnson, A.D., and Wolberger, C. (2000). Structure of the C-terminal domain of Tup1, a corepressor of transcription in yeast. EMBO J. *19*, 3016–3027.

Thompson, J.D., Higgins, D.G., and Gibson, T.J. (1994). CLUSTAL W: improving the sensitivity of progressive multiple sequence alignment through sequence weighting, position-specific gap penalties and weight matrix choice. Nucleic Acids Res. *22*, 4673–4680.

Van Duyne, G.D., Standaert, R.F., Karplus, P.A., Schreiber, S.L., and Clardy, J. (1993). Atomic structures of the human immunophilin FKBP-12 complexes with FK506 and rapamycin. J. Mol. Biol. *229*, 105–124.

Wall, M.A., Coleman, D.E., Lee, E., Iniguez-Lluhi, J.A., Posner, B.A., Gilman, A.G., and Sprang, S.R. (1995). The structure of the G protein heterotrimer G_i $\alpha_1\beta_1\gamma_2$. Cell *83*, 1047–1058.

Wilson, R.B., and Roof, D.M. (1997). Respiratory deficiency due to loss of mitochondrial DNA in yeast lacking the frataxin homologue. Nat. Genet. *16*, 352–357.

Wingert, R.A., Galloway, J.L., Barut, B., Foott, H., Fraenkel, P., Axe, J.L., Weber, G.J., Dooley, K., Davidson, A.J., Schmid, B., et al. (2005). Deficiency of glutaredoxin 5 reveals Fe-S clusters are required for vertebrate haem synthesis. Nature *436*, 1035–1039.

Yarunin, A., Panse, V., Petfalski, E., Tollervey, D., and Hurt, E. (2005). Functional link between ribosome formation and biogenesis of iron-sulfur proteins. EMBO J. *24*, 580–588.

Accession Numbers

Crystal structure coordinates of the Cia1 protein have been deposited in the Protein Data Bank with the accession code 2HES.